

Design, Modeling, and Analysis of Inductive Resonant Coupling Wireless Power Transfer for Micro Aerial Vehicles (MAVs)

Gregory M. Plaizier, Erik Andersen, Binh Truong, Xiang He, Shad Roundy and Kam K. Leang

Abstract—This paper presents the design, modeling, analysis, and experimental validation of an inductive resonant wireless power transfer (WPT) system to power a micro aerial vehicle (MAV). Using WPT, in general, enables longer flight times, virtually eliminates the need for batteries, and minimizes down time for recharging or replacing batteries. The proposed WPT system consists of a transmit coil, which can either be fixed to ground or placed on a mobile platform, and a receive coil carried by the MAV. The details of the WPT circuit design are presented. A power-transfer model is developed for the two-coil system, where the model is used to select suitable coil geometries to maximize the power received by the MAV for hovering. Analysis, simulation, and experimental results are presented to demonstrate the effectiveness of the WPT circuitry. Finally, a wirelessly powered MAV that hovers above the transmit coil is demonstrated in a laboratory setting.

I. INTRODUCTION

Recent advances in technology have enabled the development of high-performance MAVs which include fixed-wing aircraft, flapping-wing aircraft, coaxial helicopters, trirotor helicopters, and the ubiquitous quadrotor helicopters (quadcopters) [1]. These small vehicles are well suited for applications that include autonomous sensor networks for remotely detecting environmental hazards, surveillance, and search and rescue operations in areas that are dangerous to humans. One of the key challenges with MAV technology is short flight times because batteries offer a limited supply of energy. For example, the average battery life of a MAV falls between 10 and 20 minutes [2], where advances have pushed the flight time to around 30 minutes [3].

Wireless power transfer, for example through magnetic resonance coupling, is a potential method to deliver power to MAVs to address the limitations — such as short flight times — associated with carrying batteries. This method gives the MAV a constant source of power to operate, virtually eliminating the need for a battery and significantly extending flight times compared to state-of-the-art battery-operated technology. The advantages of wireless charging are that the MAV can remain operational and airborne, allowing it to be useful in complex and hostile environments where landing or recovering the MAV and changing out batteries is not practical, for example when operating around chemical spills/leaks and nuclear disaster sites. For example, the MAV can be contaminated and physical interaction with the vehicle

to change out batteries is not a safe option. Furthermore, it has been suggested that wirelessly powering a quadcopter could be useful to inspect transmission lines [4], although a working demonstration was never reported. If the charging coils are set up properly in an industrial facility, the MAV used for assembly-line inspection would never have to take an operational break to charge, but rather it could constantly fly through the “charging path” to continuously recharge.

The contribution of this paper is the detailed design, modeling, and analysis of an effective inductive resonant WPT system to specifically power a MAV and experimentally demonstrating hovering for an extended period of time. Compared to recent similar work which described the design of the power amplifier for inductive resonant coupling WPT [5], the detailed design, modeling, and analysis specific to MAV operation, to the best knowledge of the authors, has not been published. In this work, the WPT is designed through modeling to maximize the ratio of power received by the MAV to that of the power requirements for the MAV. Additionally, a sensing scheme is proposed in which the MAV can sense its location relative to the transmit coil and this information can be used to develop a feedback controller to position the MAV at the optimum location for maximum power received.

II. RELATED WORKS

The area of wireless power transfer has recently attracted the attention of researchers, in particular research in magnetic resonance coupling wireless power transfer (MRC-WPT) [6]. For example, the optimal ratio of planar spiral coil sizes in a MRC-WPT system was examined in [7]. When comparing coil size and distance for efficiency, it was reported that at closer distances, transmit (T_x) and receive (R_x) coils of similar size have higher efficiency than coils of mismatched size, but as separation distances increase, the efficiency of a small R_x coil coupled with a larger T_x coil is better than similarly sized coils. Other work has been performed to compare different coil geometries, such as planar circular spiral coils, square helical coils, and circular solenoid coils to demonstrate the effects of coil shape on efficiency with change in load and separation distance [8]. The results indicate that power transfer through planar spiral coils generally decreases more quickly due to deviations in operating frequency, as opposed to coil shape. However, planar spiral coils perform similarly to other shapes when the operating frequency is close to the resonant frequency of the coils.

The concept of resonant capacitive coupling wireless power transfer to charge and power an aerial vehicle was illustrated in a brochure by Solace Power Inc. [9]. However, this technol-

G. M. Plaizier, B. Truong, and S. Roundy are with the ISS (Integrated Self-Powered Sensing) Lab, Department of Mechanical Engineering, University of Utah, Salt Lake City, Utah 84112. E. Andersen, X. He and K. K. Leang are with the DARC (Design, Automation, Robotics and Control) Lab, University of Utah Robotics Center and Department of Mechanical Engineering, Salt Lake City, Utah 84112. Contact e-mails: shad.roundy@utah.edu and kam.k.leang@utah.edu.

ogy is sensitive to the changes in capacitance of the transmit system and the generation of potentially high voltages. On the other hand, inductive resonant linked coils, which are more robust and operate at lower voltages, have been demonstrated for WPT [5]. Recently, a simple demonstration was performed to power a MAV quadcopter, in which the T_x coil used was a clover-shape printed circuit and the R_x coil was made of copper tape which was wrapped around the quadcopter frame. However, the detailed design, modeling, and analysis of the inductive resonant WPT system specific to MAV operation, to best knowledge of the authors, was not performed and published. This paper presents new work on a detailed model-based approach to design a WPT specifically for a MAV and experimentally demonstrates its effectiveness for hovering. Additionally, a magnetic-based sensing scheme is described to allow sensing of the MAV's position relative to the transmit coil for developing feedback controllers to position the MAV at the optimum location for maximum power received. It is pointed out that related magnetic field sensing to aid aerial vehicles to locate battery charging stations has been of interest to the unmanned aerial vehicle (UAV) community. For example, magnetic fields created by transmission lines have been exploited by fixed-wing UAVs to land and recharge while inspecting areas around power lines [10]. A small scale current-carrying power line was built and theoretical simulations were used to model the UAV behavior and show that the developed control system would be sufficient to guide a small UAV to a power line based on magnetic field. In this work, magnetic field sensing is proposed to allow the MAV to determine its location relative to the power transmit coil for closed-loop control.

III. SYSTEM DESCRIPTION

The WPT system for the MAV uses resonant inductively-coupled coils as the power transmission mechanism. An RF power amplifier is used to power the transmit coil, where on the transmit (T_x) side impedance matching is in the form of an L-network. Current from the receive (R_x) coil is rectified to DC and regulated to 3.7 V for use by the MAV. The entire experimental system is shown in Fig. 1 and the equivalent circuit diagram of the WPT system is shown in Fig. 2.

In this work, the chosen MAV is a custom built drone using the frame and motors of a Jianjian Technology Co., LTD model JJRC-H98 quadcopter attached to a bitcraze crazyflie 2.0 control board, with dimensions of 14 cm by 14 cm by 9.5 cm, total weight (with battery) of 85 g.

The power amplifier used to power the system is a class E power amplifier made by Wibotic, Inc., with output impedance of 50Ω . An MFJ antenna tuner is used as an L-network impedance matching circuit. A custom-made 7-turn, 190-mm outer diameter coil made of 14-AWG copper wire is used as the transmit coil in the WPT system. Similarly, a custom-made 1-turn, 200-mm outer diameter coil made from 20-AWG magnet wire serves as the receiver. A half-bridge harmonically terminated rectifier is used to convert AC to DC [11]. A DC-DC boost-buck converter is used to regulate the voltage to 4.0 V to control the MAV. Planar

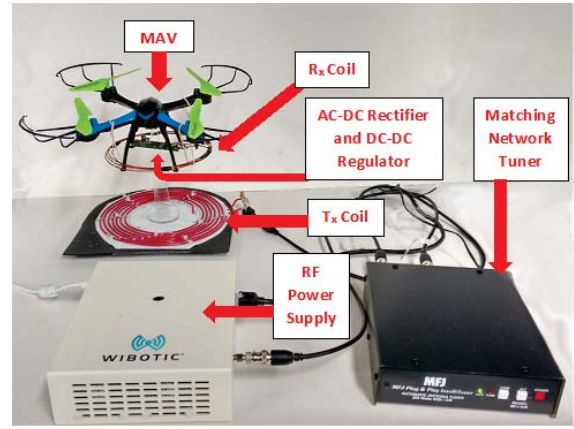


Fig. 1. The complete MAV and WPT system. The WPT system is powered using the RF power supply with frequency of 13.56 MHz. The L-circuit is used to provide impedance matching between the 50Ω source impedance and the rest of the WPT system. The transmit T_x and receive R_x coils are tuned to resonate at 13.56 MHz. The AC-DC circuit rectifies the current from the R_x coil and the DC regulator maintains 4.0 V input to the MAV.

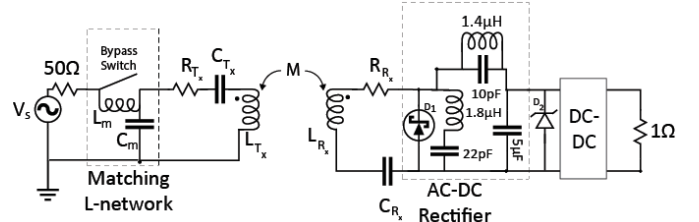


Fig. 2. The equivalent circuit diagram of the WPT system where R_s represents the source resistance, R_{T_x} and R_{R_x} represent the inherent Ohmic and radiative resistance of the T_x and R_x coils, respectively, and C_{T_x} and C_{R_x} are the tuning capacitors used to make the coil resonate at 13.56 MHz. The inductances of the coils are denoted by L_{T_x} and L_{R_x} . Parasitic capacitances of the coils are neglected.

spiral geometry is chosen for the WPT system because of the convenience of attaching to the MAV system.

Magnetic field position sensors are custom-made by winding 39-AWG coils 10 times to create loops to capture the magnetic flux when operating near the transmit coil. This flux induced a voltage that is sampled by a data acquisition system. The amplitude of the sine wave is measured, and used to infer the position of the MAV relative to the magnetic field generated by the WPT system.

IV. MODELING APPROACH

The power transfer system is simplified to a two-coil WPT model with no matching networks or power management. This work is interested in the relationship between power received by the receive R_x coil and the power required to generate lift for the MAV. This ratio, which will be defined as the figure of merit, Γ , is expressed as

$$\Gamma = \frac{P_\varepsilon}{P_\varphi}, \quad (1)$$

where P_ε is the power received at the load of the R_x coil and P_φ is the power required by the MAV to hover with the coil. The figure of merit Γ is of interest because it provides a suitable unitless value which can be used to compare many coil designs and MAV sizes.

To model the power received to the power required, the power versus thrust relationship for a selected MAV is required. The experiment involved fixing the experimental MAV

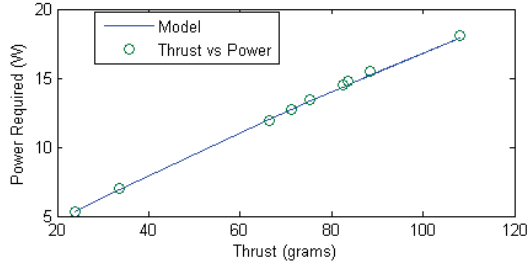


Fig. 3. The power-to-thrust relationship for the experimental MAV (Jianjian Technology Co., LTD model JJRC-H98), comparing measurements and model.

(with loaded weight of 115 g for the test) to a scale and using a DC power supply to power the MAV in place of the battery. As the throttle on the MAV was increased the change in scale measurement was recorded with the associated voltage and current. Figure 3 displays the experimentally measured power-to-thrust relationship for the MAV, along with a polynomial-fit of the data ($R^2 = 0.9994$), given by

$$P = -0.0002t^2 + 0.1759t + 1.2212, \quad (2)$$

where P is the power consumed by the MAV in Watts and t is the thrust in grams which the MAV needs for hover.

Coil design parameters include wire diameter, number of coil turns, pitch, and coil diameter. The coil model must calculate receive coil mass to use with the thrust-to-power relationship given by Eq. (2). With the density of copper as 8.96 g/cm³, the length of the coil l , self inductance L , AC resistance R_{AC} , mutual inductance M , and coupling coefficient k [7] are calculated using

$$l = \frac{1}{2}N\pi(D_o + D_i), \quad (3)$$

$$L = \frac{N^2(D_o - N(w + p))^2}{16D_o + 28N(w + p)} \times \frac{39.37}{10^6}, \quad (4)$$

$$R_{AC} = \sqrt{\frac{f\pi_o\mu_o}{\sigma}} \times \frac{N(D_o - N(w + p))}{w}, \quad (5)$$

$$M = \sum_{i=1}^{N_{T_x}} \sum_{j=1}^{N_{R_x}} \mu_o R_i R_j \times \int_0^{\pi} \frac{\cos(\Theta) d\Theta}{\sqrt{R_i^2 + R_j^2 + d^2 - 2R_i R_j \cos(\Theta)}}, \text{ and} \quad (6)$$

$$k = \frac{M}{\sqrt{L_i L_j}}, \quad (7)$$

where D_o is outside diameter of the coil, D_i is the inside diameter of the coil, N is the number of coil turns, w is the wire diameter, p is the pitch, f is the operating frequency (in this work 13.56 MHz), σ is conductivity of copper (59.6 $\times 10^6 \frac{S}{m}$), μ_o is the permeability of free space, d is the distance between the two coils, and r_i and r_j are radii of each turn for the T_x and R_x coils, respectively. In Eq. (6), coils are assumed to be coaxial and parallel-planar. When coils are not coaxial and parallel-planar mutual inductance between

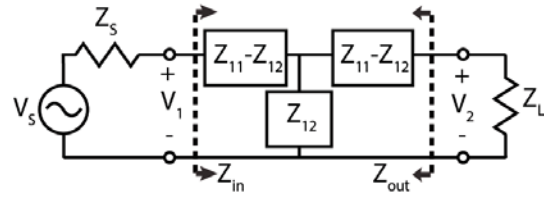


Fig. 4. The equivalent circuit model of a WPT system with a T-equivalent two-port network, where Z_{in} is the impedance seen by the RF power supply and Z_{out} is the impedance seen by the load. The T-network represents the two-port element formed by the coupled coils.

each turn is calculated using mutual inductance calculations outlined in [12] and methods from [13].

The transmit coil geometry is held constant when comparing receive coil geometries. Using the coil values found above, an impedance analysis of the system is performed to determine power delivery capabilities of each system as shown by

$$Z_{11} = R_1 + j\omega L_{T_x} + \frac{1}{j\omega C_{T_x}}, \quad (8)$$

$$Z_{22} = R_L + R_2 + j\omega L_{R_x} + \frac{1}{j\omega C_{R_x}}, \quad (9)$$

$$Z_{12} = Z_{21} = j\omega M, \text{ and} \quad (10)$$

$$Z_{in} = Z_{11} - \frac{Z_{12}^2}{Z_{22} + Z_L}. \quad (11)$$

The impedance of the WPT system, Z_{in} , as seen by the source is found using a T-equivalent two-port network as shown in Fig. 4. The T-equivalent two-port network is a representation of the simplified circuit used for modeling purposes.

By calculating the impedances throughout the WPT system, the current through the T_x coil is calculated with

$$I_1 = \frac{V_s Z_{22}}{Z_{11} Z_{22} + (\omega M)^2}, \quad (12)$$

and the current through the R_x coil is calculated with

$$I_2 = -\frac{jV_s(\omega M)}{Z_{11} Z_{22} + (\omega M)^2}. \quad (13)$$

The instantaneous power going into the T_x coil can then be calculated with

$$P_{in} = I_1^2 Z_{in}, \quad (14)$$

and the instantaneous power received at the load is calculated using

$$P_{\varepsilon} = I_2^2 R_L. \quad (15)$$

Many coil geometries are tested with these equations to determine a suitable geometry for application with the selected MAV and a fixed T_x coil geometry of 200 mm outer diameter, 10mm pitch, 6 turns, and made of 14-AWG wire. The maximum transmit power is 100 W with a maximum limit of 2 A and 50 V, which is a similar output from the power supply used in this work.

As illustrated by the results in Fig. 5, the figure-of-merit, Γ , increases with increasing pitch and decreasing number of coils. Coils with two or fewer turns are shown here to be suitable, assuming a 1.29 mm wire diameter and 150-mm outer diameter. Figure 6 shows the relationship of the change in coil diameter and change in number of turns to the power

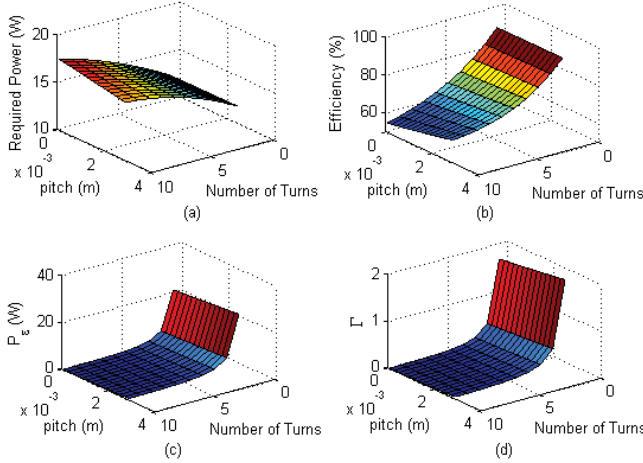


Fig. 5. Performance of the WPT system: (a) power required to lift the MAV, (b) efficiency of the WPT system, (c) power received at the load (P_e), and (d) figure-of-merit Γ . In each plot the number of R_x coil turns and pitch were varied. As the results show, fewer turns with wider spacing between turns results in a greater Γ .

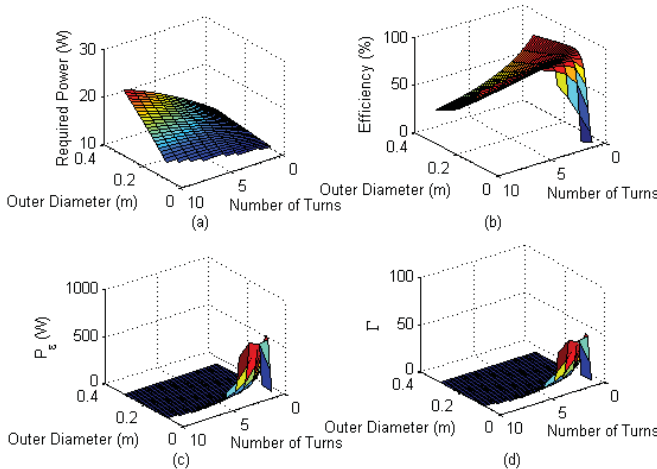


Fig. 6. An example of the relationship between number of R_x coil turns and R_x coil diameter: (a) power required to lift the MAV, (b) efficiency of the WPT system, (c) P_e , and (d) Γ , according to the modeling. As seen, the plot indicates that there is an optimal ridge to maximize the ratio of power transferred to power required.

figure of merit, Γ . The results show a ridge of optimal Γ based on the coil diameter and the number of turns. Figure 7, which shows the relationship between number of turns and wire diameter, indicates that a smaller wire diameter and fewer turns have a higher Γ . Based on the modeling results a suitable R_x coil is made with 1.29-mm diameter (16 AWG) wire, two coil turns, with an outer diameter of 130 mm and pitch of approximately 1 mm.

V. POSITIONING SENSING AND CONTROL

The MAV's small size makes it extremely susceptible to drift [14], and accurate position control relative to the wireless power transmit coil is needed to ensure that optimum power is received by the MAV. To sense the relative displacement between the MAV and transmit coil during hover, a magnetic field sensor is designed and characterized.

It has been shown that for a circular shaped T_x coil

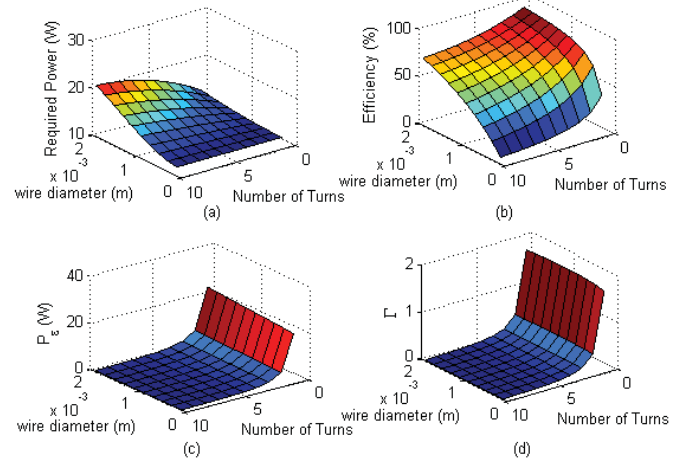


Fig. 7. An example of the effect on the Γ by the number of R_x coil turns and R_x wire diameter according to the modeling. The results shown here are (a) power required to lift the MAV, (b) efficiency of the WPT system, (c) power received at the load (P_e), and (d) Γ . These results indicate that the Γ is maximized for small wire diameters and low number of turns.

the resulting magnetic field will be a symmetrically-shaped sphere [15]. The flux of the magnetic field is strongest at the center of the coil and decreases at a rate that can be modeled as a polynomial function [16]. Because of this rapid decline in flux and hence power, it is important to avoid T_x and R_x coil misalignment and keep the MAV hovering over the T_x coil. By mapping this magnetic field and through the placement of sensors on the MAV, closed-loop feedback control can be utilized to keep the MAV above the transmit coil.

The magnetic field sensor is an induction coil sensor consisting of a 10-turn solenoid coil made of 39-AWG copper wire with a 10-mm diameter, as shown in the inset in Fig. 8. Magnetic flux from the T_x coil induces an EMF voltage according to Faraday's Law

$$\epsilon = N \times \frac{d\Phi}{dt}, \quad (16)$$

where the EMF voltage, ϵ , is directly proportional to the change in flux, Φ , which corresponds with position of the sensor in the magnetic field and the number of turns, N , on the sensor loop. The most magnetic flux, and consequently the highest sensor voltage, will pass through the sensor coil when it is directly centered above the T_x coil. Through experimental measurements at 11.5 cm above the transmit coil, the output voltage of the sensor as a function of radial distance from the center of the coil is shown in Fig. 8. Thus, at a given vertical distance, z , the displacement of the sensor coil in the x/y plane can be empirically modeled by

$$e_s(H)|_z = a_2 H^2 + a_1 H + a_0, \quad (17)$$

where H is the radial distance from the center of the T_x coil to the sensor and $e_s|_z$ is the EMF sensor voltage at a given vertical distance z . Using Eq. (17), the horizontal radial distance of the sensor on the MAV relative to the center of the T_x coil can be approximated and used for position estimation. A design is proposed where four sensors can be placed on the MAV. Three sensors are placed in a triangular configuration each located 60 mm from the center of the MAV.

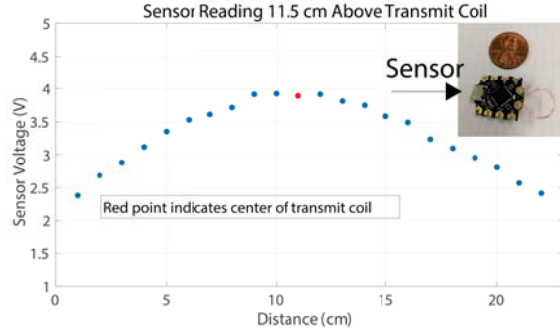


Fig. 8. The magnetic position sensor (inset) and a plot of the sensor readings as a function of radial distance from the center of the transmit coil measured at 11.5 cm above the coil. The center of the T_x coil is located at 11 cm.

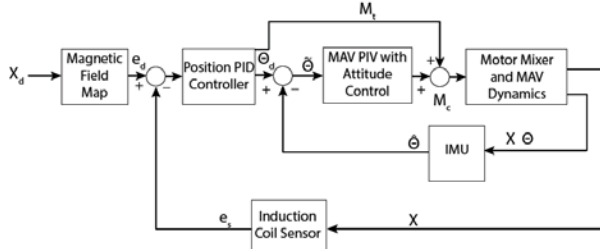


Fig. 9. The block diagram of the control system enabling the MAV to hover in place above the transmit coil of the WPT using the custom-designed magnetic position sensor.

The fourth sensor can be placed in the center of the MAV. The three sensors in the triangular configuration can be used to approximate the gradient of the magnetic field.

Using the sensor output, a feedback controller as illustrated in Fig. 9 can be used to control the position of the MAV to hover at an optimum location relative to the transmit coil. This effort is mapped by the controller into a vector $\Theta_d = [\phi_d, \theta_d, \psi_d]$, which contains the Euler angles of roll, pitch and yaw, respectively, and a motor output proportional to the thrust M_t . The vector Θ is compared in negative feedback loop with $\hat{\Theta}$, the estimate of the Euler angles from the MAV's IMU. The resulting vector is passed into the MAV's internal attitude controller. The output of the attitude controller is then summed with M_t to form inputs to the individual motors. It is noted that this controller will keep the MAV hovering above the T_x coil but it will not be able to control the yaw or horizontal orientation of the MAV relative to the T_x coil. Additional sensors are required to measure and control the yaw motion. However, since the received power of the MAV is not dependent on its horizontal orientation, the controller will keep the MAV in a position to receive the required power.

VI. EXPERIMENTAL RESULTS AND DISCUSSION

This section demonstrates WPT to the experimental MAV system described above in Section III. The T_x coil is made of seven turns and 5-mm pitch with 190 mm outer diameter using 14-AWG copper wire. The R_x coil is made of a 200 mm diameter, single turn loop using 20-AWG magnet wire. The R_x coil, rectifier, and DC-DC converter have a mass of 22 g and the MAV consumes approximately 14.7 W to hover with the additional mass of the coil and electronics. The power input to the WPT system was approximately 40 W, with 36%

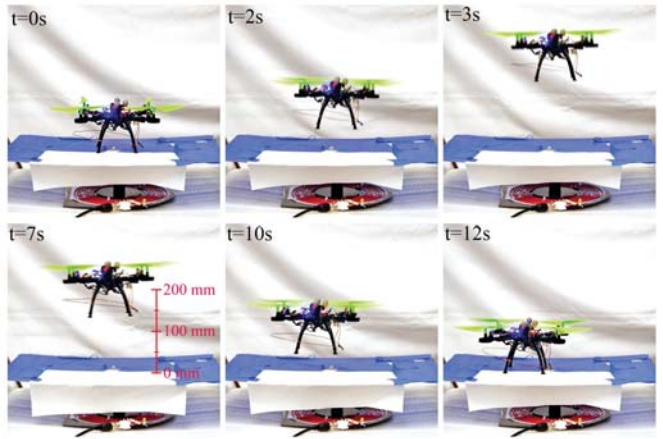


Fig. 10. A working demonstration of the MAV as it hovers using the WPT system, where the MAV is resting on a platform suspended above the T_x coil by 80 mm and the MAV hovering receiving power and taking off of the platform, and hovering approximately 120 mm above the T_x coil.

TABLE I
THEORETICAL AND EXPERIMENTAL VALUES OF A 13.7-CM COIL WITH 1-MM PITCH, 2 TURNS, AND 1.29-MM DIAMETER WIRE

| | Theoretical | Experimental | % deviation |
|----------------------|-------------|--------------|-------------|
| L_{R_x} (μ H) | 1.19 | 1.40 | 16.2 |
| C_{R_x} (pF) | 115.7 | 93.0 | 21.5 |
| N_{R_x} | 2 | 2 | 0 |
| pitch (mm) | 1 | 1 | 0 |
| D_o (mm) | 137 | 137 | 0 |
| Coil Sep. (mm) | 100 | 100 | 0 |
| f_o (MHz) | 13.56 | 13.24 | 2.4 |
| P_e (W) | 16.91 | 15.2 | 10.65 |
| P_{in} (W) | 18.07 | 18 | 0.39 |
| R_L (Ω) | 12.5 | 12.5 | 0 |

efficiency.

Figure 10 shows still frames of the MAV as it takes off and hovers from a platform suspended above the transmit coil. The platform is 80 mm from the T_x coil and the MAV hovers for an extended period of time approximately 120 mm from the T_x coil. For this demonstration the MAV's position is controlled through a motion capture system (OptiTrack). Three IR markers were placed on the MAV, enabling the motion capture system to track the MAV's position. The MAV's position was compared in a negative feedback loop with the desired position, and the resulting error was fed into a PID position control loop through a custom built ROS program designed for the Crazyflie 2.0 flight controller allowing the MAV to hover above the T_x coil.

To further validate the model, two R_x coils were constructed and tested using a resistive load. The power conditioning electronics and impedance matching tuning were removed from the system to more closely replicate the modeling approach discussed in this work. The summary of the results are found in Tables I and II.

The results shown in the tables indicate that the model is able to reasonably estimate inductance values for coils. In the model, resonating capacitor values are calculated based on the desired resonant frequency and neglect self capacitance of the coil. However, experimentally the self capacitance of the coils has an increasing effect on resonant frequency as

TABLE II

THEORETICAL AND EXPERIMENTAL VALUES OF A 15.3-CM COIL WITH 2-MM PITCH, 4 TURNS, AND 1.29-MM DIAMETER WIRE

| | Theoretical | Experimental | % deviation |
|-----------------------|-------------|--------------|-------------|
| L_{Rx} (μ H) | 4.4 | 4.6 | 4.4 |
| C_{Rx} (pF) | 31.5 | 24.3 | 25.8 |
| N_{Rx} | 4 | 4 | 0 |
| pitch (mm) | 2 | 2 | 0 |
| D_o (mm) | 153 | 153 | 0 |
| Coil Sep. (mm) | 100 | 100 | 0 |
| f_o (MHz) | 13.56 | 13.27 | 2.2 |
| P_e (W) | 15.33 | 9 | 52.5 |
| P_{in} (W) | 16.0 | 16 | 0 |
| R_L (Ω) | 12.5 | 12.5 | 0 |

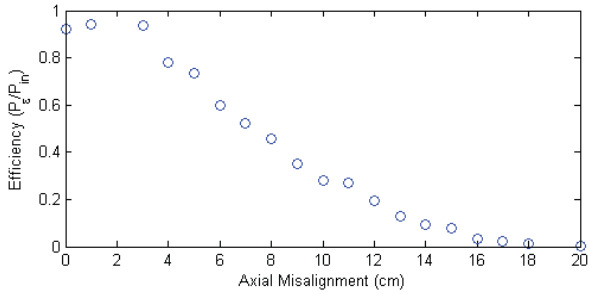


Fig. 11. Plot of how power efficiency at the load through the WPT system is affected by distance from axial alignment between T_x and R_x coils. Because the R_x coil is smaller than the T_x coil the plot has a small plateau around axial alignment, which indicates that there is approximately a 4-cm radius for which the MAV could move horizontally and still receive sufficient power.

number of coil turns and coil inductance increases. Therefore, experimentally, capacitor values are selected to tune the resonant frequency coil close to the operating frequency. The power delivered to the load matched well for the first R_x coil but had a larger error with the second R_x coil. In the case of the 4-turn R_x coil, if the measured inductance and resonant frequency are used to calculate the capacitance, and the theoretical inductance and calculated capacitance used in the model, then the theoretical P_e is calculated to be 11.9 W, which results in a percent deviation from experimental of 27.8%.

To determine the sensitivity of the WPT to the MAV's location, the R_x coil is terminated by a 12.5Ω resistor and power efficiency is mapped as the R_x coil moves from axial alignment with the T_x coil. No impedance tuning circuits were used for this test. The results of the mapping are shown in Fig. 11. This demonstrates the margin of error that the control system has, which is used to position the MAV to where it can receive enough power.

VII. CONCLUSIONS

This paper described the design, modeling, analysis, and experimental demonstration of an inductive resonant WPT system sufficient for a MAV to hover. Using a two-coil WPT model, the geometry for the T_x and R_x coil was chosen based on simulated performances. The model was validated through experimental results and a proof-of-concept was demonstrated by successfully powering a MAV, enabling it to hover. Additionally, a sensing and control system that would allow the MAV to remain within the WPT charging path was proposed. Future work will focus on validating the

proposed control system based on the WPT field, investigating different coil materials as well as additional coil geometries (*i.e.*, square, solenoid, etc.), and the use of multiple R_x coils on the MAV.

VIII. ACKNOWLEDGMENTS

This material is based upon work supported, in part, by the University of Utah and the National Science Foundations Partnership for Innovation Program (Grant No. 1430328). Any opinions, findings, and conclusions or recommendations expressed in this material are those of the authors and do not necessarily reflect the views of the sponsors.

REFERENCES

- [1] V. Kumar and N. Michael, "Opportunities and challenges with autonomous micro aerial vehicles," *Int. J. of Robotics Research*, vol. 31, no. 11, pp. 1279 – 1291, 2012.
- [2] A. Abdilla, A. Richards, and S. Burrow, "Power and endurance modelling of battery-powered rotorcraft," in *Intelligent Robots and Systems (IROS), 2015 IEEE/RSJ International Conference on*, Hamburg, Germany, Sept. 2015, pp. 675–680.
- [3] J. A. Benito, G. G. de-Rivera and Javier Garrido, and R. Ponticelli, "Design considerations of a small uav platform carrying medium payloads," in *Proc. 2014 Conference on Design of Circuits and Integrated Circuits (DCIS)*, Nov. 2014, pp. 1–6.
- [4] M. Simic, C. Bil, and V. Vojisavljevic, "Investigation in wireless power transmission for UAV charging," *Procedia Comput. Sci.*, vol. 60, pp. 1846–1855, Sept. 2015.
- [5] S. Aldhaher, D. C. Yates, and P. D. Mitcheson, "Design and development of a class of 2 inverter and rectifier for multimegahertz wireless power transfer systems," *IEEE Trans. Power Electron.*, vol. 31, pp. 8138–8150, Dec. 2016.
- [6] A. Kurs, A. Karalis, R. Moffatt, J. Joannopoulos, P. Fisher, and M. Soljacić, "Wireless power transfer via strongly coupled magnetic resonances," *Science*, vol. 317, no. 5834, pp. 83–86, July 2007.
- [7] B. H. Waters, B. J. Mahoney, G. Lee, and J. R. Smith, "Optimal coil size ratios for wireless power transfer applications," in *Proc. IEEE International Symposium on Circuits and Systems (ISCAS'14)*, Melbourne, Australia, June 2014, pp. 2045–2048.
- [8] X. Shi, C. Qi, M. Qu, S. Ye, G. Wang, L. Sun, and Z. Yu, "Effects of coil shapes on wireless power transfer via magnetic resonance coupling," *Journal of Electromagnetic Waves and Applications*, vol. 28, no. 11, pp. 1316–1324, 2014.
- [9] *Keeping UAVs in the Air with Wireless Power*, Solace Power, 2016.
- [10] J. Moore and R. Tedrake, "Magnetic localization for perching UAVs on powerlines," in *IEEE/RSJ International Conference on Intelligent Robots and Systems IROS*, San Francisco, CA, USA, Sept. 2011.
- [11] A. Ganti, J. Lin, R. A. Chinga, and S. Yoshida, "Harmonically terminated high-power rectifier for wireless power transfer," *Wireless Power Transfer*, vol. 3, no. 2, pp. 75–82, 2016.
- [12] F. W. Grover, "The calculation of the mutual inductance of circular filaments in any desired positions," in *Proc. IRE*, Oct. 1944, pp. 620–629.
- [13] S. Babic, F. Sirois, C. Akyel, and C. Girardi, "Mutual inductance calculation between circular filaments arbitrarily positioned in space: Alternative to grover's formula," *IEEE Trans. Magn.*, vol. 63, pp. 3591–3600, Sept. 2010.
- [14] S. Weiss, R. Brockers, and L. Matthies, "4dof drift free navigation using inertial cues and optical flow," in *Intelligent Robots and Systems (IROS), 2013 IEEE/RSJ International Conference on*. IEEE, 2013, pp. 4180–4186.
- [15] J. Kim, J. Kim, S. Kong, H. Kim, I.-S. Suh, N. P. Suh, D.-H. Cho, J. Kim, and S. Ahn, "Coil design and shielding methods for a magnetic resonant wireless power transfer system," *Proceedings of the IEEE*, vol. 101, no. 6, pp. 1332–1342, 2013.
- [16] D. Liu, H. Hu, and S. V. Georgakopoulos, "Misalignment sensitivity of strongly coupled wireless power transfer systems," *IEEE Transactions on Power Electronics*, vol. 32, no. 7, pp. 5509–5519, 2017.